

NONLINEAR OPTICAL PHENOMENA https://doi.org/10.1070/QEL16286

Room- and low-temperature transmission of diffusion-doped Fe^{2+}:ZnSe polycrystal at 2940 nm

N.N. Il'ichev, G.A. Bufetova, E.S. Gulyamova, P.P. Pashinin, A.V. Sidorin, V.I. Polyanskii, V.P. Kalinushkin, E.M. Gavrishchuk, V.B. Ikonnikov, D.V. Savin

Abstract. **Transmission of a polycrystalline Fe^{2+}:ZnSe sample during irradiation by a pulsed Er^{3+}:YAG laser with a wavelength of 2940 nm is measured at low and room temperatures. It is found that the sample in a strong field (energy density 1.3 J cm^{-2}, laser pulse duration 320 ns, peak intensity 4.1 MW cm^{-2}) is bleached almost completely at both low and room temperatures. The temperature dependence of transmission is measured in the range of 105–273 K in weak and strong fields.**

Keywords: *Fe^{2+}: ZnSe, nonlinear transmission, low temperature.*

1. Introduction

At present, there is a need for high-power solid-state lasers emitting in the wavelength range of 4000–5000 nm. One of the active materials for these lasers is ZnSe crystal doped with Fe^{2+} [1].

The nonlinear transmission of this material as a function of the energy density of high-power pulsed radiation was measured in works [2–7], in which transmission was found to increase with increasing radiation energy density. The measurements in [2–5, 7] were performed at room temperature, while the measured temperatures in [6] were higher (up to 220 °C). Since the decay time of luminescence from the upper level of Fe^{2+} in ZnSe crystals strongly depends on temperature (105 μs at 120 K [1] and 355 ns at 300 K [8]), it is of interest to measure nonlinear transmission of Fe^{2+}:ZnSe crystals at low temperatures. The present work is devoted to measuring nonlinear transmission of Fe^{2+}-doped CVD-grown ZnSe crystal at low temperature. Such measurements have not been performed previously. We also present the results of measurement of nonlinear transmission of this crystal at room temperature.

AN.N. Il'ichev, G.A. Bufetova, E.S. Gulyamova, P.P. Pashinin, A.V. Sidorin, V.P. Kalinushkin A.M. Prokhorov General Physics Institute, Russian Academy of Sciences, ul. Vavilova 38, 119991 Moscow, Russia; e-mail: ilichev@kapella.gpi.ru;
V.I. Polyanskii Moscow Institute of Physics and Technology (State University), Institutskii per. 9, 141701 Dolgoprudnyi, Moscow region, Russia; A.M. Prokhorov General Physics Institute, Russian Academy of Sciences, ul. Vavilova 38, 119991 Moscow, Russia;
E.M. Gavrishchuk, V.B. Ikonnikov, D.V. Savin G.G. Devyatykh Institute of Chemistry of High-Purity Substances, Russian Academy of Sciences, ul Tropinina 49, 603950 Nizhnii Novgorod, Russia

Received 17 January 2017
Kvantovaya Elektronika **47** (2) 111–115 (2017)
Translated by M.N. Basieva

2. Setup for measuring nonlinear transmission

Figure 1 shows the optical scheme for transmission measurement. Substrate (*1*) deflected part of Er^{3+}:YAG laser radiation to PD29 photodetector (*2*), which measured the radiation incident on the sample. A telescope consisting of CaF_2 lenses (*3*) and (*4*) with focal lengths f = 300 and 100 mm, respectively, formed a beam with a required diameter in Fe^{2+}:ZnSe sample (*7*). To attenuate the radiation, we used filter (*5*); the sample was placed in cryostat (*6*) with CaF_2 windows. The focused laser beam was incident on sample (*7*) at an angle of 27°; the sample was positioned in the focal plane of CaF_2 lens (*8*) (f = 150 mm). Attenuating NS9 filter (*9*) (transmission 1/200) was placed as shown in Fig. 1 in the case of measurements in a strong field and replaced to the position of filter (*5*) in front of cryostat (*6*) for weak-field measurements. CaF_2 lens (*10*) (f = 150 mm) was placed behind filter (*9*). In the focal plane of lens (*10*), we placed a light diffuser made of 14 GGG-crystal plates, each of them being 450 μm thick and 5 mm in diameter, which were placed one after another in a copper tube polished inside. PD29 photodetector (*11*) measured the radiation passed through the sample. BaF_2 lenses (*12*) and (*14*) (f = 100 mm) formed the image of the irradiated region on PD47 photodetector (*15*), which was used to measure the luminescence or laser radiation with a wavelength in the region of 4–5 μm. The pump radiation was blocked by filter (*13*) with a low transmission at a wavelength of 2940 nm and a high transmission at wavelengths within the range of 3500–5000 nm. The radiation incident on the sample was linearly polarised by Glan prism (*16*) so that the electric field vector lied in the plane of incidence of radiation on the sample.

The actively Q-switched Er^{3+}:YAG laser had a transverse radiation distribution close to the TEM_{00} mode, a wavelength

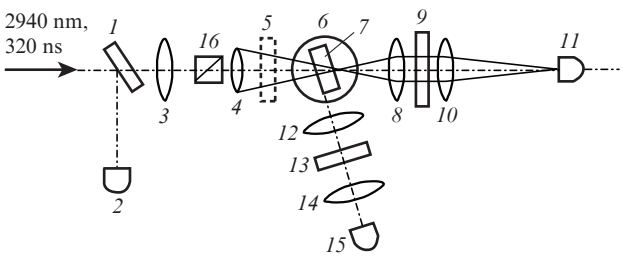

Figure 1. Optical scheme for measuring the transmission of samples.

of 2940 nm, and a pulse duration of about 320 ns; the Gaussian beam cross section at the entrance to the sample was 11.17×10^{-3} cm^2 (beam radius 0.027 cm); and the radiation energy was 2.0–2.2 mJ. The peak energy density (in the transverse distribution maximum) inside the sample reached 1.33 J cm^{-2}, while the peak intensity was 4.1 MW cm^{-2}. Since the angle of incidence of the beam on the sample was 27°, in our calculations we took into account the difference between the beam cross sections at the entrance to the sample and inside it.

The transmissions measured at a high radiation power are denoted below as strong-field measurements by the letter s. The transmissions measured with attenuated radiation [with filter (*9*) in position (*5*)] are denoted as weak-field measurements by the letter w.

The electric signals were recorded on a Tektronix DPO 7254 oscilloscope with a bandwidth of 2.5 GHz. The oscilloscope input impedance was 50 Ω.

We studied transmission of a polycrystalline Fe^{2+}:ZnSe sample with the size of $20 \times 20 \times 3$ mm, which was fabricated according to the following procedure. First, the polished surface of a ZnSe sample synthesised by the CVD method was coated by an iron film in a flow reactor at a temperature of 610–620 °C in an Ar flow in the reaction between iron chloride and zinc vapours ($FeCl_2 + Zn \rightarrow Fe + ZnCl_2$). Then, the sample was annealed at a high temperature (1000 °C) in an evacuated quartz ampoule in a zinc atmosphere for 72 h. The optical transmission of the sample at a wavelength of 2940 nm after chemomechanical polishing was ~30% taking into account the Fresnel reflection. The doped layer thickness calculated from the known diffusion coefficient of Fe^{2+} in ZnSe ($D = 7.95 \times 10^{-10}$ cm^2 s^{-1} at 1000 °C [9] taking into account its approximately twofold increase as a result of annealing in zinc vapours [10]) did not exceed 600 μm. The effective concentration of iron ions determined from the absorption spectrum of the sample taking into account its thickness was $\sim 1.5 \times 10^{18}$ cm^{-3}. The concentration of the other controlled impurities in the sample determined by the ICP-AS method did not exceed 10^{-4} wt %.

The sample was placed in an optical cryostat. To eliminate the effect of the interference of radiation reflected from the optical facets of the crystal on the measurement results, the angle of incidence of radiation on the sample was chosen to be about 27°. The occurrence or absence of lasing or superluminescence in the plane of the entrance face of the sample under the action of high-power radiation was controlled by a system of lenses (*12*) and (*14*), which formed the image of the sample face on the input window of a PD47 photodetector (see Fig. 1).

3. Procedure of signal measurement and processing

The sample transmission was measured as follows. First, we measured the signals u_{01} and u_{02} from photodetectors (*2*) and (*11*), respectively. From these signals, we subtracted their constant components u_{01} and u_{02} and thus obtained the signals $U_1 = u_1 - u_{01}$ and $U_2 = u_2 - u_{02}$. Then, using the Fourier transform, we excluded all high-frequency components with frequencies exceeding the intermode beat frequency. After this, the inverse Fourier transform was performed. As a result, we obtained signals U_{f1} and U_{f2}. In the absence of a sample, the maxima of the U_{f1} and U_{f2} signals were superimposed using a programme for selecting the delay between the signals. This delay was unchanged when processing the measurement results. The signals at each time moment were divided by each other, and this ratio ($r = U_{f2}/U_{f1}$) was determined in the cases of presence (r_1) and absence (r_0) of the sample. Then, the transmission was determined as $T = r_1/r_0$.

4. Results of measurements of nonlinear transmission

Figure 2 presents the time dependences of transmission in the absence of a sample (100% line) for weak (peak intensity 0.015 MW cm^{-2}) and strong (peak intensity 2.0 MW cm^{-2}) fields. One can see that these curves deviate from 100% by no more than 1% for the entire pulse duration time. Figure 2 also shows the intensities of the input (I_{in}) and output (I_{out}) signals measured by photodiodes (*2*) and (*11*) and normalised to the intensity maximum, which almost completely coincide.

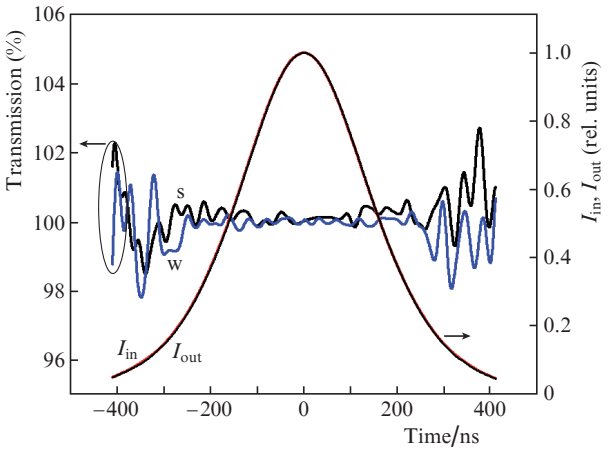

Figure 2. Time dependence of the setup transmission without a sample (100% transmission line) for weak (w) and strong (s) fields, as well as input (I_{in}) and output (I_{out}) signals normalised to the maximum radiation intensity.

Figure 3 shows the time dependences of the transmission of a CVD-grown Fe^{2+}:ZnSe sample at room temperature (295 K) in weak and strong fields. The input energy densities in the strong field were 1.3 and 0.4 J cm^{-2}, the latter value being obtained due to attenuation of radiation by a BS7 filter (transmission 30%) placed in front of lens (*3*) (see Fig. 1). These energy densities at the entrance to the sample were chosen both to obtain additional information and control the experimental accuracy. It should be noted that high-power radiation forms a thermal lens in the sample. To exclude the influence of the thermal lens on the signal of photodiode (*11*), the image of the irradiated region of the sample was formed on the input plane of a diffuser placed in front of the receiving area of the photodiode. The presence of the diffuser ensured that the small shifts of the beam spot on its input plane, which may occur due to the change of the position of filter (*9*), did not influence the signal value. Figure 3 also shows the input and output radiation intensities normalised to the maximum, which are noticeably different. The dashed curves in Fig. 3 show the calculated curves of the sample transmission at the aforementioned input energy densities. A characteristic feature of the strong-field transmission is the existence of a maximum on the transmission curve. This is explained by the fact

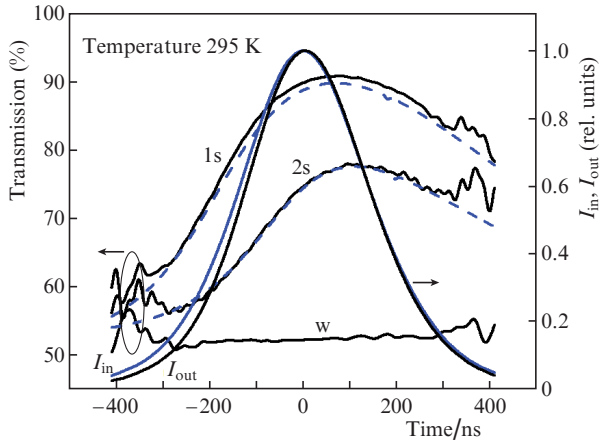

Figure 3. Time dependences of the sample transmission at room temperature in weak (w) and strong (s) fields at the input energy densities of 1.3 (1s) and 0.4 (2s) J cm^{-2}, as well as input (I_{in}) and output (I_{out}) signals normalised to the maximum radiation intensity. The dashed curves correspond to the calculated time dependences of transmission at the same input energy densities.

that the lifetime of the upper level of Fe^{2+} in ZnSe at room temperature (340 ns [8]) is comparable with the laser pulse duration (320 ns).

Figure 4 presents the time dependences of the sample transmission at a temperature of 105 K in strong and weak fields at the input energy densities of 1.3 and 0.4 J cm^{-2}, as well as the intensities of the input and output signals normalised to the radiation intensity maximum and the calculated transmission curves at the same input energy densities. The transmission curves in strong fields at low temperature are characterised by a monotonic growth during the pulse duration. This occurs because the lifetime of the upper level of Fe^{2+} in ZnSe at a temperature of 105 K is about 100 μs [1], i.e., considerably longer than the laser pulse duration.

In the measurements of transmission at temperatures of 295 and 105 K, the absence of lasing along the optical plane

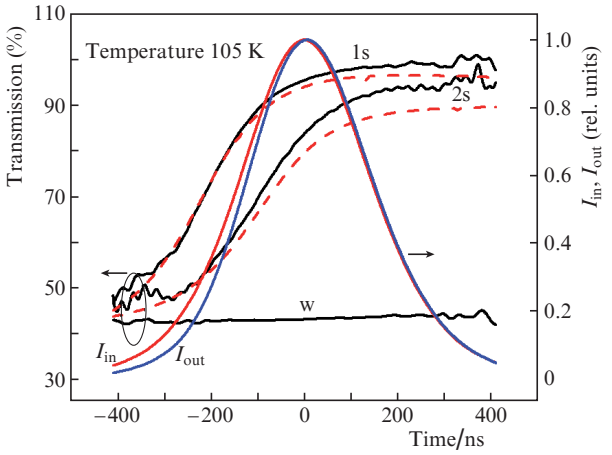

Figure 4. Time dependences of the sample transmission at a temperature of 105 K in strong (s) and weak (w) and fields at the input energy densities of 1.3 (1s) and 0.4 (2s) J cm^{-2}, as well as input (I_{in}) and output (I_{out}) signals normalised to the maximum radiation intensity. The dashed curves show the calculated time dependences of the transmission at the same input energy densities.

of the sample was controlled using photodiode (*15*) (see Fig. 1).

It is of interest to discuss the behaviour of the lower Fe^{2+} level population averaged over the crystal length during the action of high-power radiation. This population is proportional to $\ln(T/T_0)$, where T is the sample transmission and T_0 is the transmission in a weak field. We processed the transmission dependences shown in Figs 3 and 4 and plotted the dependence of $\ln(T/T_0)$ on the energy density at the entrance to the sample

$$E = \int_{-\infty}^{\tau} I_{in}(x)\,dx$$

(where τ is the time) at T_0 = 43% (105 K) and 53% (295 K). These dependences are shown in Fig. 5 together with the curves calculated at the aforementioned input energy densities.

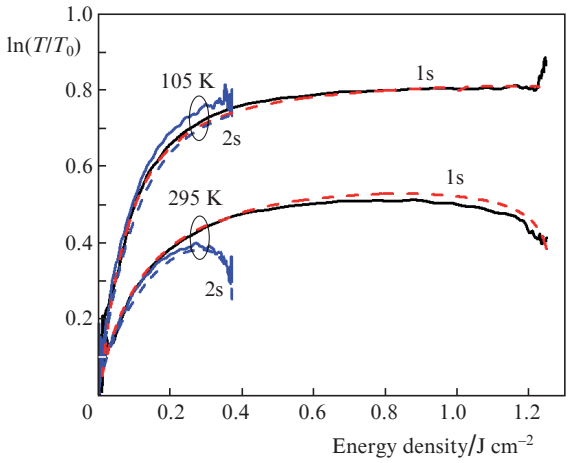

Figure 5. Dependences of $\ln(T/T_0)$ on the energy density at the entrance to the sample at room temperature and 105 K for input energy densities of 1.3 (1s) and 0.4 (2s) J cm^{-2}, as well as calculated dependences at the same input energy densities (dashed curves).

The temperature dependences of the sample transmission in strong and weak fields upon heating the sample from 105 to 273 K are shown in Fig. 6. The transmission was measured

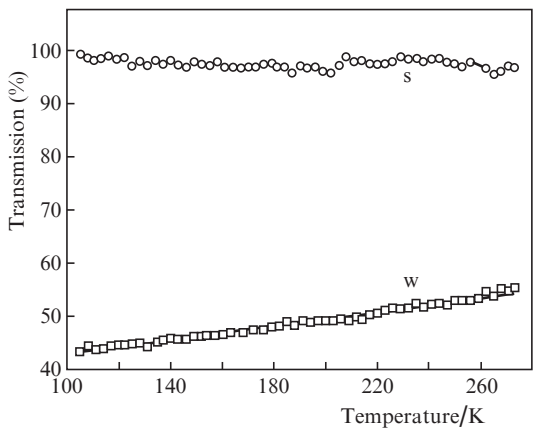

Figure 6. Temperature dependences of the sample transmission in strong and weak fields at the input energy densities of 1.3 J cm^{-2} (s) and 6 mJ cm^{-2} (w).

as the ratio of the amplitudes of pulses passed through the sample and incident on it, which was normalised to the corresponding ratio in the absence of the sample. One can see that the transmission is almost independent of temperature in the strong field (average value 97%) but monotonically increases in the weak field.

The experimental data on the sample transmission in the $\ln(1/T)$–temperature coordinates are well described by a linear function. This dependence of transmission is related to a decrease in the absorption cross section with increasing temperature. Processing of the experimental data shows that the absorption cross section at a wavelength of 2940 nm decreases with increasing temperature according to the law $\sigma(t) = \sigma(t_0)[\gamma(t_0 - t) + 1]$, where $\gamma = 2.3 \times 10^{-3}$ K^{-1}, $t_0 = 295$ K, and t is the temperature in kelvins.

5. Discussion of results

The radiation intensity I in the sample and the population n_1 of the lower Fe^{2+} level in ZnSe are well described by the well-known equations for pulse propagation in a three-level medium with absorption saturation (see, for example, [11, 12]). In this scheme, radiation is resonantly absorbed by a centre at a certain transition and then the excitation energy nonradiatively (for a time on the order of picoseconds and shorter) decays to a lower-lying level, the lifetime of which in our case is several hundreds of nanoseconds at room temperature and several tens of microseconds at liquid nitrogen temperature (it is assumed that the excited centre does not interact with the high-power radiation):

$$\frac{\mathrm{d}I}{\mathrm{d}z} = -\sigma n_1 I, \tag{1a}$$

$$\frac{\mathrm{d}n_1}{\mathrm{d}\tau} = -\sigma n_1 I + \frac{n_0 - n_1}{\tau_{ex}}, \tag{1b}$$

where n_0 is the concentration of Fe^{2+} ions in a particular region of the crystal, σ is the absorption cross section at the radiation wavelength, and τ_{ex} is the lifetime of the upper level. It is assumed that radiation interacts only with unexcited centres and that the pulse duration considerably exceeds the time of light propagation through the sample. The weak-field transmission T_0 is related to the ion concentration n_0 by the expression

$$\ln T_0 = -\int_0^L \sigma n_0 \mathrm{d}z,$$

while the transmission in a strong field is described by the relation

$$\ln T = -\int_0^L \sigma n_1 \mathrm{d}z.$$

Then, the change in the lower level population during the pulse action is

$$\ln\frac{T}{T_0} = \int_0^L \sigma(n_0 - n_1)\,\mathrm{d}z. \tag{2}$$

From (1a), (1b) and (2), we obtain the expression for the time dependence of transmission:

$$\frac{\mathrm{d}}{\mathrm{d}\tau}\ln T = \sigma I_{in}(1 - T) - \frac{1}{\tau_{ex}}\ln\frac{T}{T_0}. \tag{3}$$

Equations (2) and (3) were used to calculate the time dependences of transmission. The calculations were performed on the assumption that the transverse intensity distribution at the entrance to the sample is Gaussian, i.e., $I_{in} \propto \exp[-2(r/w)^2]$, where r is the radius and $w = 0.029$ cm ($S = 1.28 \times 10^{-3}$ cm^2). The time dependence of the radiation intensity at the entrance to the sample was described as $I_{in} \propto [\cosh(\tau/\tau_1)]^{-1}$, where $\tau_1 = 122$ ns, which corresponds to a pulse FWHM of 320 ns. The intensity at the entrance to the sample was determined for each time moment as a function of the transverse coordinate measured from the centre of the transverse distribution. Using Eqn (3), we found the intensity at the output from the sample at the same time moment. The transmission was determined as the ratio between the output and input powers. The power was determined by summing the intensities over the sample cross section multiplied by the element area. Such determination of transmission corresponds to the experimental conditions when the photodetector signal is proportional to the radiation power.

The absorption cross section of the sample at a wavelength of 2940 nm at room temperature was taken to be $\sigma = 10^{-18}$ cm^2 [1]. The cross section at a temperature of 105 K calculated from the measured transmissions in a weak field at room and low temperatures was found to be $\sigma = (1.3 \pm 0.1) \times 10^{-18}$ at 2940 nm. In calculation we also used the lifetimes of 390 ns at room temperature and 100 μs at low temperature.

The calculation results are shown in Figs 3–5 by dashed lines. One can see that the calculated curves well describe the experimental data in both transmission–time and $\ln(T/T_0)$–input energy density coordinates.

Note also that neither the absorption from the excited state nor the nonresonance absorption was taken into account in calculations. The existence of a maximum on the transmission curves at room temperature (see Figs 3, 5) is explained by the fact that the laser pulse duration is comparable with the lifetime of the upper level of Fe^{2+}.

6. Conclusions

(1) The transmission of a CVD-grown Fe^{2+}:ZnSe sample is measured during the action of a high-power radiation pulse at a wavelength of 2940 nm at room temperature. It is found that the time dependence of the transmission has a maximum.

(2) The transmission of a sample of the same crystal is measured during irradiation by a high-power 2940-nm pulse at a temperature of 105 K. It is found that the time dependence of the transmission has no maximum and the transmission monotonically increases during the pulse action.

(3) The transmission curves calculated in the model of a three-level medium with absorption saturation well describe the experimental data at both room and low temperatures. The calculation was performed taking into account the transverse radiation distribution.

(4) The maximum transmission of a Fe^{2+}:ZnSe sample for high-power radiation at both room and low temperatures is close to 100%, which indicates the absence of nonresonance absorption in the sample.

(5) The temperature dependence of the sample transmission is measured within the range of 105–273 K. The strong-

field transmission is close to 100% and is almost independent of temperature, while the weak-field transmission linearly increases with temperature, which is related to a decrease in the 2940-nm absorption cross section with increasing temperature t according to the law $\sigma(t) = \sigma(t_0)[\gamma(t_0 - t) + 1]$ with $\gamma = 2.3 \times 10^{-3}$ K^{-1} and $t_0 = 295$ K.

Acknowledgements. This work was partially supported by the Russian Foundation for Basic Research (Project Nos 16-02-00807a, 15-52-45024 IND-a, and 15-59-31817 PT-omi).

References

1. Adams J.J., Bibeau C., Page R.H., et al. *Opt. Lett*., **24** (23), 1720 (1999).
2. Kisel V.E., Shcherbitskii V.G., et al. *Zh. Prikl. Spektrosk*., **72** (6), 747 (2005).
3. Il'ichev N.N., Shapkin P.V., et al. *Laser Phys*., **17** (2), 130 (2007).
4. Cankaya H., Demirbas U., Erdamar A.K., Sennaroglu A. *J. Opt. Soc. Am. B*, **25** (5), 794 (2008).
5. Gallian A., Martinez A., Marine P., et al. *Proc. SPIE Int. Soc. Opt. Eng*., **6451**, 64510L-1 (2007).
6. Il'ichev N.N., Pashinin P.P., Gulyamova E.S., et. al. *Quantum Electron*., **44** (3), 213 (2014) [*Kvantovaya Elektron*., **44** (3), 213 (2014)].
7. Bufetova G.A., Gulyamova E.S., Il'ichev N.N., et al. *Quantum Electron*., **45** (6), 521 (2015) [*Kvantovaya Elektron*., **45** (6), 521 (2015)].
8. Akimov V.I., Voronov A.A., Kozlovskii V.I., et al. *Quantum Electron*., **36** (4), 299 (2006) [*Kvantovaya Elektron*., **36** (4), 299 (2006)].
9. Demirbas U., Sennaroglu A., Somer M. *Opt. Mater.*, **28** (3), 231 (2006).
10. Gafarov O., Martinez A., Fedorov V., Mirov S. *Opt. Mater. Express*, **7** (1), 25 (2017).
11. Il'ichev N.N. *Principles of solid-state lasers. Handbook of Solid-State Lasers: Materials, Systems And Applications*. Ed. by B. Denker, E. Shklovsky (Woodhead Publishing Series in Electronic and Optical Materials, 2013) No. 35, pp 171–192.
12. Koechner W. *Solid State Laser Engineering* (New York: Springer Science+Media Inc., 2006).